JOURNAL OF MATERIALS SCIENCE 31 (1996) 5499–5504

Crack formation and oxidation in superplastically deformed Si_3N_4

N. KONDO, F. WAKAI
National Industrial Research Institute of Nagoya, Hirate-cho, Kita-ku, Nagoya, Aichi 462, Japan

Crack formation and oxidation during superplastic deformation of Si_3N_4 were studied and the superplastic forming ability of Si_3N_4 was discussed. Tensile deformation tests were conducted under a 1 atm nitrogen atmosphere at 1600 °C, and under a constant crosshead speed with an initial strain rate of $2 \times 10^{-5}\,s^{-1}$. The microstructures of superplastically deformed specimens were observed by SEM. The relation between chemical composition and microstructure was determined by EPMA. After 280% deformation (at fracture), the formation of regions rich in glassy phase was observed. These regions, supposed to be formed due to oxidation of cracks, appeared just before fracture. The present material is capable of being deformed up to strains of 210%.

1. Introduction

Commonly, a uniform microstructure with very fine equiaxed grains is required for achievement of superplasticity, because equiaxed grains are preferable to grain-boundary sliding which is a major mechanism of superplasticity. However, from recent works [1, 2], the superplasticity of Si_3N_4 was found to be not peculiar to the microstructure of fine and equiaxed grains, but that Si_3N_4 with a microstructure containing elongated β-Si_3N_4 grains, can be superplastic.

One of the most important features of superplastic deformation of Si_3N_4 is the obvious microstructure change during deformation. Before deformation, elongated β-Si_3N_4 grains are randomly oriented. However, after deformation, elongated grains align with their long axis preferentially along the tensile axis. The rotation of elongated grains during superplastic deformation brings about this microstructure. Anisotropic grain growth also accompanies the deformation. The observation of grain growth clearly shows mass transport through a solution–precipitation process. This fact suggests that the solution–precipitation creep can take place as an accommodation process of grain-boundary sliding in superplasticity.

True stress shows unusual strain hardening during deformation. This increment of true stress is assumed to be the result of grain reorientation and growth. Usually, an increment of true stress causes crack formation, followed by fracture. Furthermore, in the case of superplastically deformed Si_3N_4, oxidation of cracks occurs and glassy phase-rich regions are formed inside the cracks, bridging the cracks which extend inside the specimen.

The existence of cracks and glassy phase-rich regions should have a bad effect on the mechanical properties of superplastically deformed Si_3N_4. Thus, it is important for manufacturing applications of superplastic forming to clarify the cracking and the oxidation mechanism. In this report, we study the crack formation and the oxidation during superplastic deformation and discuss the superplastic forming ability of Si_3N_4.

2. Experimental procedures

The sample was prepared by gas pressure sintering, with 5 wt % Y_2O_3 and 3 wt % Al_2O_3 as additives. Its density was $3.2 \times 10^3\,kg\,m^{-3}$, and its bending strength and fracture toughness were 1100 MPa at room temperature and 5.7 $MPa\,m^{1/2}$, respectively. Further information on the fabrication and the mechanical properties are reported elsewhere [3]. According to the results of chemical analysis, the sample contained 3.7 wt % Y, 1.7 wt % Al, and 3.5 wt % O. (The sample used in this report is the same as SN2 reported earlier [2]. It exhibited superplastic elongation of about 280%.)

Tensile test specimens were cut from the sintered body, ground rotationally by diamond wheels and polished by diamond pastes. They had a gauge length of 10 mm and a circular cross-section of 3 mm diameter. Uniaxial tensile deformation tests were performed using a universal testing machine (Model 1361, Instron, USA) equipped with SiC fixtures and a furnace with tungsten mesh heating elements. The deformation tests were conducted under a 1 atm nitrogen atmosphere at 1600 °C, and under a constant crosshead speed with an initial strain rate of $2 \times 10^{-5}\,s^{-1}$. The specimens were heated to 1600 °C at a rate of $30\,°C\,min^{-1}$. The deformation tests were started after holding the specimens for 10 min to allow homogenization of the internal temperature. After deformation, the specimens were cooled at a rate of $60\,°C\,min^{-1}$ to below 1000 °C.

0022–2461 © *1996 Chapman & Hall*

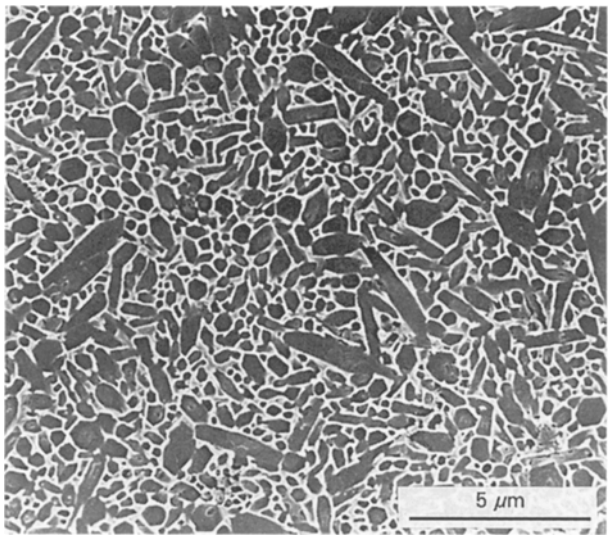

Figure 1 Scanning electron micrograph of the specimen before deformation.

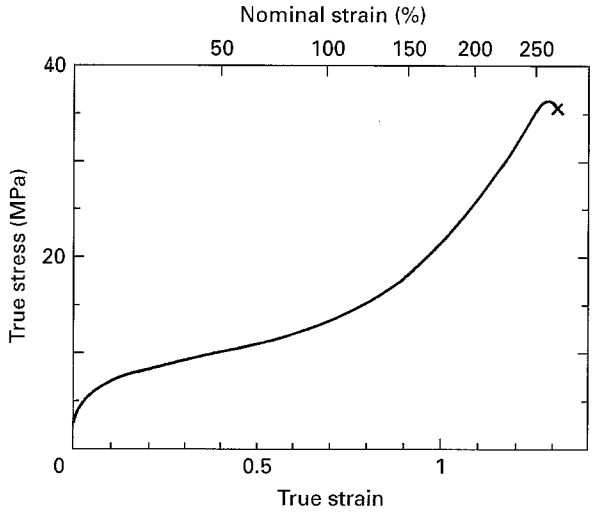

Figure 2 The stress–strain curve of the superplastically deformed specimen. $T = 1600\,°C$; $\dot{\varepsilon}_0 = 2 \times 10^{-5}\,s^{-1}$.

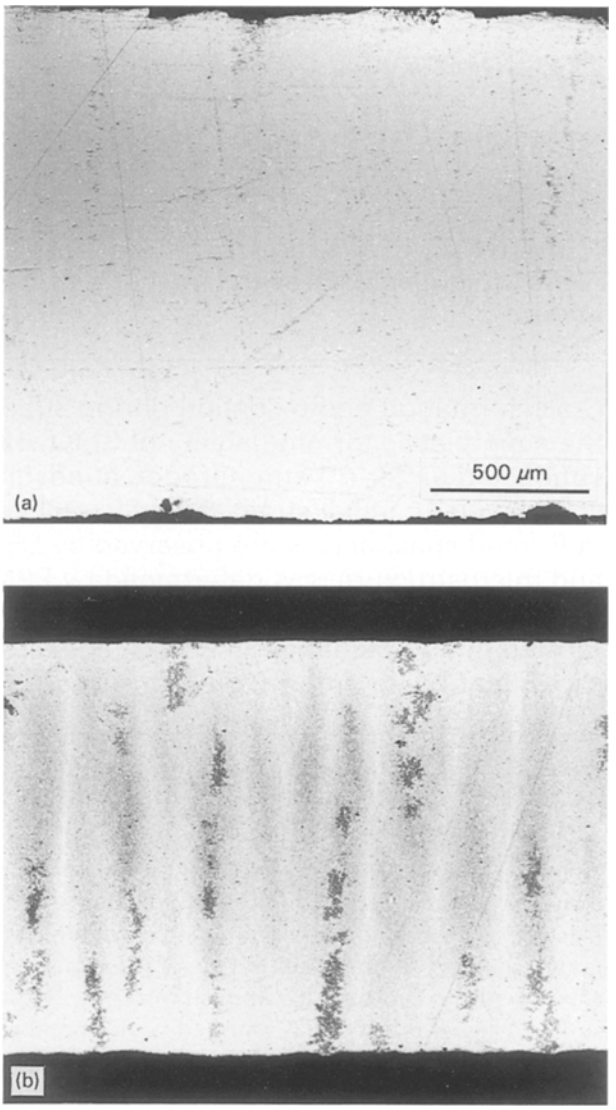

Figure 3 Optical micrographs of the superplastically deformed specimen. (a) 210% deformed specimen (not fractured); (b) 280% deformed specimen (fractured). Black areas correspond to the glassy phase-rich regions; the tensile direction is horizontal.

SEM observations were conducted to examine microstructures of as-sintered specimens and that of a superplastically deformed specimen using a JSM-5200 (Jeol, Japan). SEM specimens were ground, polished and plasma etched by CF_4, followed by gold coating.

Electron probe microanalysis (EPMA) observations of the superplastically deformed specimen was performed to determine the relation between chemical composition and microstructure using a JCXA-773 (Jeol, Japan) with a wavelength dispersive spectrometer (WDS). The EPMA specimen was ground and polished, followed by carbon coating.

3. Results

Fig. 1 shows a scanning electron micrograph of the microstructure of the specimen before deformation. The specimen consists of randomly oriented elongated β-Si_3N_4 grains. The average diameter of grains (grain size) is about 0.4 μm and the apparent aspect

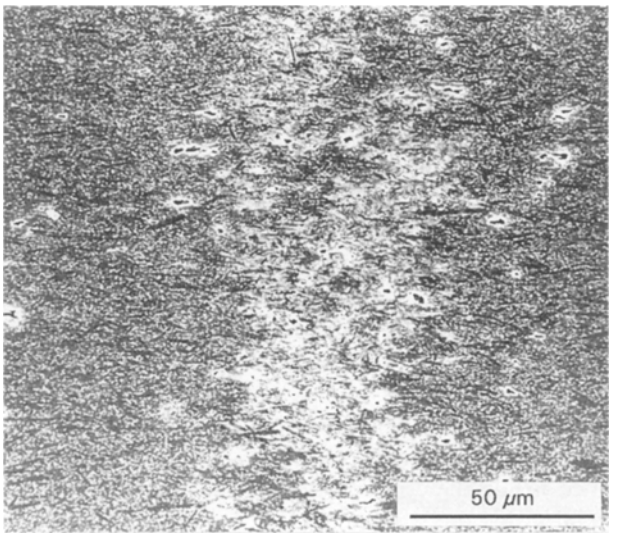

Figure 4 Scanning electron micrograph of the 280% superplastically deformed specimen. This micrograph shows the whole view of the glassy phase-rich region. The tensile direction is horizontal.

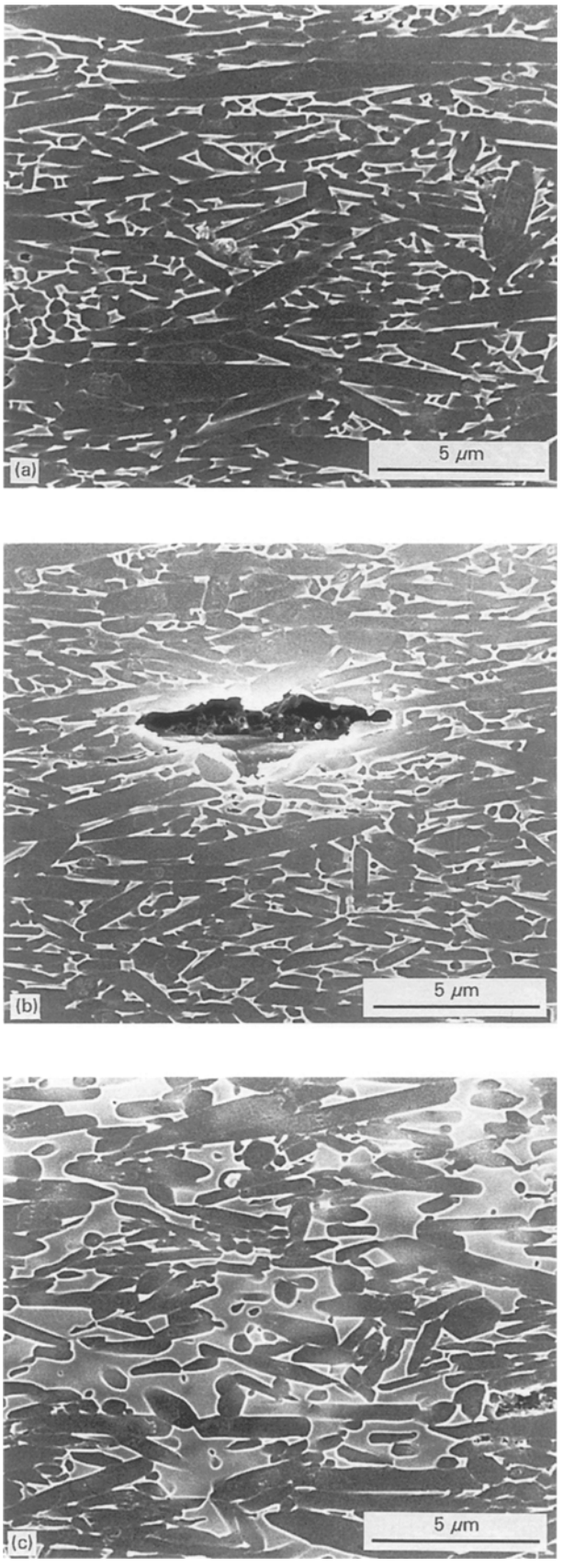

Figure 5 Scanning electron micrographs of the 280% superplastically deformed specimen. These micrographs each show a magnified area of Fig. 4. (a) β-Si_3N_4 grain-rich region (black area of Fig. 4); (b) cavity; (c) glassy phase-rich region (white area of Fig. 4). The tensile direction is horizontal.

ratio is about 3.5. This specimen had a uniform microstructure, and no heterogeneous distribution of glassy phase was observed.

The true stress–true strain curve of the tensile test is shown in Fig. 2. The specimen was superplastically deformed up to 280%. At the first stage of deformation, the specimen was deformed under a true stress of lower than 10 MPa. However, the true stress was gradually increased during deformation and reached 37 MPa just before fracture.

Many cracks were observed on the cylindrical gauge surface of the 280% deformed tensile specimen (fractured), and a thin oxide scale was formed on the surface of the specimen. The specimen in which deformation was stopped at an elongation of 210% (not fractured) was also observed. No cracks were observed on its surface.

Fig. 3b shows an optical micrograph of the 280% deformed specimen. This micrograph was taken from the specimen which was prepared for SEM observation. It shows a cross-section parallel to the tensile direction. Some black bands, which lie perpendicular to tensile direction, are observed. The black bands shown in this micrograph extended into the specimen from the surface cracks. The 210% deformed specimen was also observed, but no such bands were found (Fig. 3a). To examine these black bands, we performed SEM observations. Fig. 4 shows a whole view of one of those black bands. In this micrograph, the black band shown in Fig. 3b corresponds to the white region. Fig. 5a is a micrograph taken from the black region of Fig. 4. This region was filled with β-Si_3N_4 grains. (We call this region the β-Si_3N_4 grain-rich region.) The long axis of these grains was preferentially aligned along the tensile axis. The average diameter of the elongated grains increased to about 0.5, and the apparent aspect ratio was also increased to about 4. As shown in Fig. 5b, some cavities were observed in this fractured specimen. There were 1–2 cavities in every 500 μm^2. The cavities were isolated and elongated along the tensile axis. No linkage of cavities could be found, although they were located close to each other. On the other hand, a micrograph taken from the white region of Fig. 4 is shown in Fig. 5c. In this region, a mass of glassy phase was surrounded by β-Si_3N_4 grains. (We call this region the glassy phase-rich region.)

In addition, EPMA observations were performed to determine the difference in chemical composition between the β-Si_3N_4 grain-rich regions and the glassy phase-rich regions. A back-scattered electron image of the specimen is shown in Fig. 6a. The white areas correspond to the glassy phase-rich regions. Characteristic X-ray images of YK_α, AlK_α and OK_α are shown in Fig. 6b, c and d, respectively. Each figure was taken from the same area. Note that as the density of dots does not reflect the amount of elements exactly, we can only discuss qualitative properties. The glassy phase-rich region contained a larger amount of yttrium in comparison with the β-Si_3N_4 grain-rich region. Oxygen also was concentrated in the glassy phase, but compared with yttrium there was a smaller difference between the glassy phase-rich region and the β-Si_3N_4 grain-rich region. In contrast, aluminium was distributed uniformly in both regions.

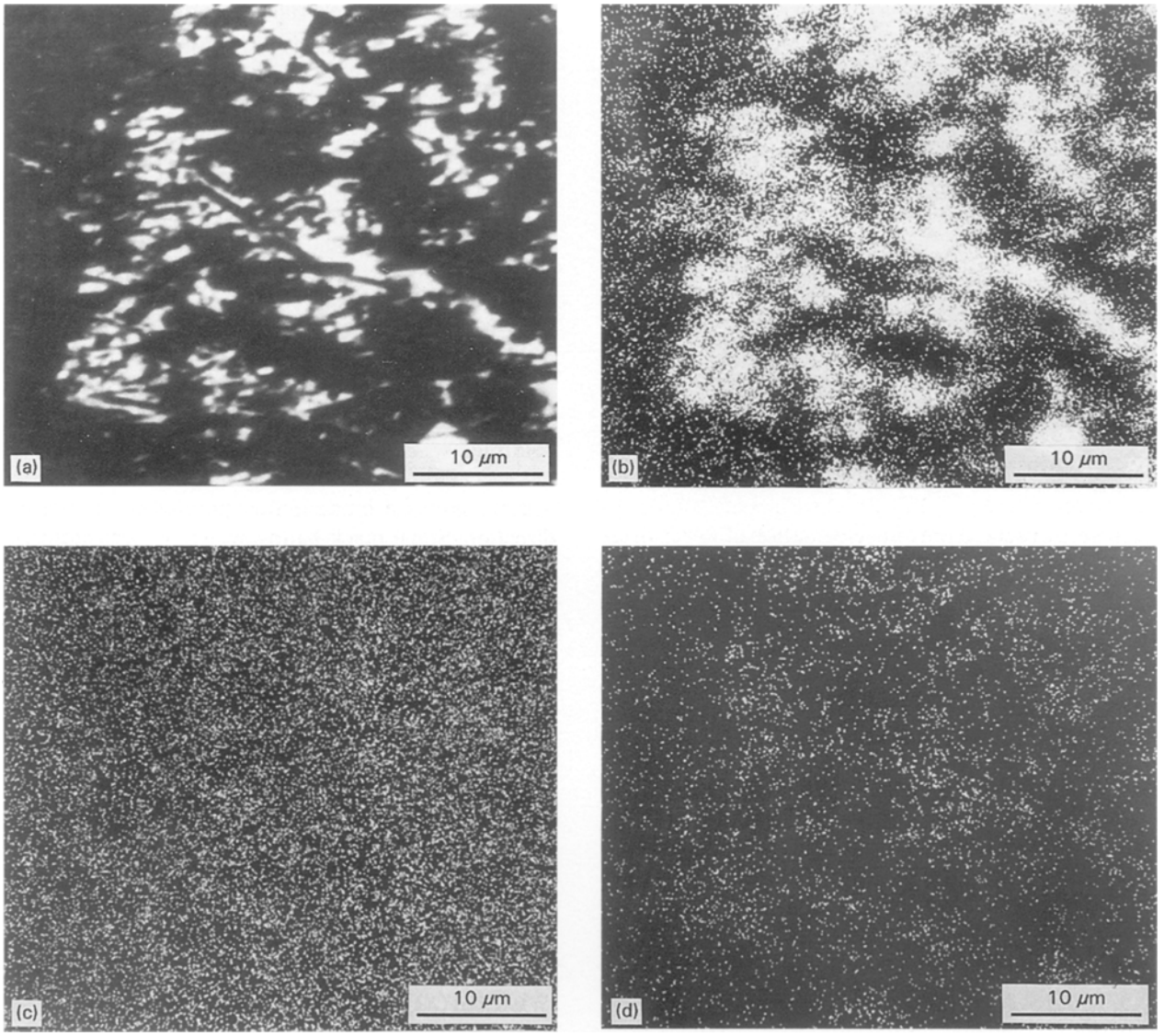

Figure 6 EPMA images of the superplastically deformed specimen. (a) Back-scattered electron image (white areas correspond to glassy phase-rich regions); (b) YK_α characteristic X-ray image; (c) AlK_α characteristic X-ray image; (d) OK_α characteristic X-ray image. The tensile direction is horizontal.

4. Discussion

Reorientation of grains in specimens which are superplastically deformed in tension has already been described [1, 2, 4, 5], but the formation of a glassy phase-rich region was observed for the first time in this specimen. Usually, Si_3N_4 ceramics are produced by a liquid-phase sintering process. Sintering aids, such as Y_2O_3, Al_2O_3 and MgO, which form a eutectic liquid with Si_3N_4 at high temperature, are added to bring about liquid-phase sintering. This liquid phase forms a glassy grain-boundary phase. Our material also contains glassy grain-boundary phase.

The results show that the bands of glassy phase-rich regions were developed in the 280% deformed specimen. There is insufficient evidence to determine the quality of the glassy phase formed after superplastic deformation. However, here we assume from circumstantial evidence such as phase diagrams, glass formation maps and chemical composition, that firstly from chemical analysis, this material consists of elements silicon, nitrogen, yttrium, aluminium and oxygen; secondly, from the results of EPMA observations, the glassy phase consists of yttrium, aluminium and oxygen; thirdly from phase diagrams [6–9], the system Si–N–O–Y–Al forms a eutectic melt at 1600 °C; and fourthly, from glass formation maps [10, 11], the eutectic melt exists as glassy phase at room temperature. Accordingly, we assume that the glassy phase should be Y–SiAlON glass.

On the other hand, neither surface cracks nor glassy phase-rich regions were observed in the specimen in which deformation was stopped at 210% elongation. Thus, the glassy phase-rich region seemed to be formed just before fracture. Furthermore, they extended into the specimen from the surface cracks and lay perpendicular to tensile direction. This suggests that the glassy phase-rich regions are formed inside the cracks.

Crack formation during superplastic deformation in silicon nitride-based ceramics was reported by Rouxel *et al.* [4]. In their case, the specimen deformed at 1600 °C had a smooth surface. However, the surface

of the specimen deformed at 1625 °C was covered with many cracks, which is similar to ours. Their results suggested that crack formation is enhanced by a chemical alteration of the surface at higher temperature, and careful selection of test conditions will result in an undamaged specimen after deformation. Our material also indicated evidence of oxidation. The oxide scale formed on the surface of the specimen was due to attack by the oxygen which remained in the furnace. Although the testing conditions of our material were the same as those of Rouxel *et al.*, our material was exposed to high temperature for more than twice as long a time. So, we suggest that our material should show more severe oxidation (and accompanying chemical alteration) than that of Rouxel *et al.*

Crack formation in crept specimens was also reported elsewhere [12–14]. Cracks which are similar to ours were observed only in deformation at lower stresses (several tens of MPa) in the creep test. This crack formation is followed by slow crack growth, linking-up of cracks and failure [13]. The crack growth is very sensitive to a small difference in stress. Elongation without cracking is possible at low stress, for example, the specimen deformed up to 210% at stresses lower than 30 MPa. However, as the deformation stress increased due to microstructural development, cracks were formed in the specimen fractured at 280% and 37 MPa.

Besides cracks, cavities were also observed in the superplastically deformed specimen. The cavities were isolated, and did not link up to each other. In most superplastic ceramics, cavitation followed by linkage of cavities lead to fracture [15, 16]. However, it is not assumed that the linkage of cavities lead to fracture in superplastic silicon nitride ceramics. The strongly oriented microstructure will prevent the linkage of cavities or crack propagation perpendicular to the tensile axis.

The oxidation of cracks observed in crept silicon nitrides in air is reported elsewhere [17–19]. In the typical case of Si_3N_4-based ceramics, glassy oxidation phase is observed in the cracks. The glassy phase covers the surface inside the cracks and bridges the cracks at the crack tips [17]. However, in our case, the glassy phases filled the whole inside of the cracks and formed glassy phase-rich regions. It seems that because our testing temperature was higher, oxidation and diffusion were activated sufficiently to form glassy phase and to fill cracks. These glassy phase-rich regions work as glassy phase bridges. As deformation stress during superplastic deformation is lower, the glassy phase bridges can support the stress without fracture.

The migration of yttrium towards the surface of crept specimens accompanying oxidation has also been observed [20–22]. Silica-rich scale on the surface of a specimen is produced by oxidation. A chemical concentration gradient causes the diffusion of yttrium from the grain-boundary glassy phase to the oxide scale. A similar diffusion mechanism is assumed to act on the glassy phase formed inside cracks. Thus, the glassy phase contained yttrium.

From the above discussion, the mechanisms of cracking and formation of glassy phase-rich regions were considered to be as follows. The increment of deformation stress caused by microstructural development and the oxidation in high temperature, caused cracks to form at the surface of the specimen. The cracks propagated inside the specimen without fracture, due to the low deformation stress. Oxidation inside the cracks forms a glassy phase-rich region, and yttrium diffuses into the glassy phase-rich regions.

5. Conclusion

The crack formation and oxidation during superplastic deformation of Si_3N_4 were studied. The formation of cracks occurred just before fracture. The increment of deformation stress caused by microstructural development and the oxidation at high temperature, induced crack formation at the surface of the specimen. The cracks propagate inside the specimen without fracture due to the low deformation stress. Oxidation inside the cracks forms a glassy phase-rich region, and yttrium diffuses into the glassy phase-rich region.

On the other hand, no crack formation was observed in the 210% deformed specimen. Furthermore, the strongly oriented microstructure is supposed to prevent crack propagation perpendicular to the tensile axis. Thus, we conclude that our material is useful for deformations lower than 210%.

Finally, the mechanical properties of the superplastically deformed specimen with strongly oriented microstructure are interesting. Further details of these studies will be discussed in another paper.

References

1. N. KONDO F. WAKAI, T. NISHIOKA and A. YAMAKAWA, *J. Mater. Sci. Lett.* **14** (1995) 1369.
2. N. KONDO, F. WAKAI, M. YAMAGIWA, T. NISHIOKA and A. YAMAKAWA, *Mater. Sci. Eng.* **A206** (1996) 45.
3. T. NISHIOKA, K. MATSUNUMA, T. YAMAMOTO, A. YAMAKAWA and M. MIYAKE, SAE Technical Paper 920384 (1992).
4. T. ROUXEL, F. WAKAI and K. IZAKI, *J. Am. Ceram. Soc.* **75** (1992) 2363.
5. X. WU and I.-W. CHEN, *ibid*, **75** (1992) 2733.
6. "Phase Diagrams for Ceramists, Volume V", edited by R. S. Roth, T. Negas and L. P. Cook (American Ceramic Society, Columbus, OH, 1983), Figs 6181 and 6182.
7. "Phase Diagrams for Ceramists, Annual '91" edited by A. E. McHale (American Ceramic Society, Westerville, OH, 1991) Figs 91–436.
8. M. WISNUDEL and T.-Y. TIEN, *J. Am. Ceram. Soc.* **77** (1994) 2653.
9. Z.-K. HUANG and T.-Y. TIEN, *ibid.* **77** (1994) 2763.
10. M. J. HYATT and D. E. DAY, *ibid.* **70** (1987) C283.
11. A. MAKISHIMA, Y. TAMURA and T. SAKAINO, *ibid.* **61** (1978) 247.
12. T. OHJI and Y. YAMAUCHI, *ibid.* **76** (1993) 3105.
13. B. J. HOCKEY, S. M. WIEDERHORN, W. LIU, J. G. BALDONI and S.-T. BULJAN, *J. Mater. Sci.* **26** (1991) 3931.
14. M. K. FERBER and M. G. JENKINS, *J. Am. Ceram. Soc.* **75** (1992) 2453.
15. D. J. SCHISSLER, A. H. CHOKSHI, T. G. HIGH and J. WADSWORTH, *Acta. Metall. Mater.* **39** (1991) 3227.
16. Y. MA and T. G. LANGDON, *ibid.* **42** (1994) 2753.

17. J. E. RITTER, K. JAKUS, M. H. GODIN and R. RUH, *J. Am. Ceram. Soc.* **75** (1992) 1760.
18. Y. G. GOGOTSI and G. GRATHWOHL, *J. Mater. Sci.* **28** (1993) 4279.
19. *Idem, J. Am. Ceram. Soc.* **76** (1993) 3093.
20. M. H. LEWIS and P. BARNARD, *J. Mater. Sci.* **15** (1980) 443.
21. A. BOUARROUDJ, P. GOURSAT and J. L. BESSON, *ibid.* **20** (1985) 1150.
22. J. CRAMPON, R. DUCLOS and N. RAKOTOHARISIA, *ibid.* **28** (1993) 909.

Received 19 January
and accepted 24 April 1996